

From 3-Hz P Waves to ${}_0S_2$: No Evidence of A Slow Component to the Source of the 2011 Tohoku Earthquake

EMILE A. OKAL¹

Abstract—In the hours following the 2011 Honshu event, and as part of tsunami warning procedures at the Laboratoire de Géophysique in Papeete, Tahiti, the seismic source of the event was analyzed using a number of real-time procedures. The ultra-long period mantle magnitude algorithm suggests a static moment of 4.1×10^{29} dyn cm, not significantly different from the National Earthquake Information Center (NEIC) value obtained by W -phase inversion. The slowness parameter, $\Theta = -5.65$, is slightly deficient, but characteristic of other large subduction events such as Nias (2005) or Peru (2001); it remains significantly larger than for slow earthquakes such as Sumatra (2004) or Mentawai (2010). Similarly, the duration of high-frequency (2–4 Hz) P waves in relation to seismic moment or estimated energy, fails to document any slowness in the seismic source. These results were confirmed in the ensuing weeks by the analysis of the lowest-frequency spheroidal modes of the Earth. A dataset of 117 fits for eight modes (including the gravest one, ${}_0S_2$, and the breathing mode, ${}_0S_0$) yields a remarkably flat spectrum, with an average moment of 3.5×10^{29} dyn cm (≈ 1.07). This behavior of the Tohoku earthquake explains the generally successful real-time modeling of its teleseismic tsunami, based on available seismic source scaling laws. On the other hand, it confirms the dichotomy, among megaquakes ($M_0 > 10^{29}$ dyn cm) between regular events (Nias, 2005; Chile, 2010; Sendai, 2011) and slow ones (Chile, 1960; Alaska, 1964; Sumatra, 2004; and probably Rat Island, 1965), whose origin remains unexplained.

Key words: Tohoku earthquake, slow components, seismological quantification, mega earthquakes.

1. Introduction

This paper uses a number of simple, robust algorithms to explore the question of the possible existence of a slow component in the source of the 2011 Tohoku earthquake. We conclude that none is present.

A general, and remarkable, property of the seismic source is the fact that it can be scaled, over as many as 17 orders of magnitude in seismic moment (IDE and BEROZA, 2001), using laws of similitude which can relate the detailed properties of the source (e.g., seismic slip and fault length), to a single expression of its size, namely the seismic moment M_0 . This observation, documented in the 1960s by AKI (1967), was already inherent in GUTENBERG and RICHTER'S (1954) discovery of frequency-magnitude relations, which were later explained theoretically, based precisely on scaling laws (RUNDLE, 1989). In turn, those relations have been at the core of the estimation of repeat times, and therefore of the quantification of seismic hazard. In simple terms, scaling laws express the physically invariant nature of the physical properties of the medium involved in the rupture, such as strength of material, rupture velocities, or stress drop.

While the overwhelming majority of earthquakes do seem to follow scaling laws, it has become apparent, as early as the 1970s, that a number of events are obvious violators. Their study, and the understanding of the context in which such violations can occur, is particularly important in the framework of tsunami warning, which to this day proceeds from an extrapolation to ultra-low frequencies (typically below 1 mHz) of a real-time seismic estimate generally obtained at periods no longer than 250 s. Indeed, KANAMORI (1972) introduced the concept of the so-called “tsunami earthquakes”, whose tsunamis are much larger than expected from their seismic magnitudes, especially conventional ones. Later work has indicated that such events were characterized by extremely slow source rupture, itself controlled by anomalous material properties at the source, in the

¹ Department of Earth and Planetary Sciences, Northwestern University, 1850 Campus Drive, Evanston, IL 60208, USA. E-mail: emile@earth.northwestern.edu

form of either sedimentary material featuring deficient mechanical properties (FUKAO, 1979; LAY and BILEK, 2007), or jagged ruptures affecting the propagation of the rupture along the fault (TANIOKA *et al.*, 1997). Both scenarios would obviously lead to violation of the tacit assumptions defining seismic similitude.

In this context, it has been observed that some of the very largest earthquakes exhibit significant slow components to their source, indicating violation of scaling laws. The largest earthquake ever recorded, the 1960 Chilean event, has long been documented to possess a slow precursory component to its source, evidenced through its clearly non-causal signature (with respect to the mainshock) on the Benioff strainmeter at Pasadena (KANAMORI and CIPAR, 1974; Fig. 3), and supported by later models proposed by KANAMORI and ANDERSON (1975), CIFUENTES and SILVER (1989) and LINDE and SILVER (1989). The 2004 Sumatra earthquake, arguably the second largest, also exhibits significant slowness, as evidenced by the strong disparity between its classical CMT solution (3.95×10^{29} dyn cm) computed around 300 s, and the definitive value of its low-frequency moment ($1\text{--}1.2 \times 10^{30}$ dyn cm), computed from ultra-long period mantle waves or the normal modes of the Earth (TSAI *et al.*, 2005; STEIN and OKAL, 2005). This property is further documented by its deficient energy-to-moment ratio (CHOY and BOATWRIGHT, 2007). A modern re-investigation of the 1964 Alaska earthquake has also led to an upwards re-evaluation of its moment, to a figure essentially identical with that of the 2004 Sumatra earthquake (NETTLES *et al.*, 2005). As the three largest quantified earthquakes do exhibit source slowness, the question naturally arises whether this property is shared by *all* “mega-quakes” (which can be defined grossly as those with $M_0 \leq 10^{29}$ dyn cm), although as pointed out in earlier works, neither the 2005 Nias earthquake, nor the 2010 Maule event, feature a slow source (STEIN and OKAL, 2005; OKAL *et al.*, 2012). The recent 2011 Tohoku event provides an opportunity to further explore this question; we conclude that the earthquake does not feature source slowness in its low-frequency spectrum.

The present study is composed of two parts. Real-time measurements presented in Sects. 2–4 were all taken as the author happened to be visiting the

Laboratoire de Géophysique of the Commissariat à l’Energie Atomique in Papeete, which serves as the Tsunami Warning Center for French Polynesia; such investigations were critical as they led, in real-time, to the conclusion that initial estimates of the seismic source could legitimately be used in the forecasting of the tsunami, in the context of the warning to be issued in that territory, reached by the waves 11.5 h after origin time. Detailed operational aspects can be found in a companion paper (REYMOND *et al.*, 2012). By contrast, the definitive seismological quantification of the source at ultra-low frequencies had to be deferred by close to one month (OKAL, 2011), as it relies on the analysis of the Earth’s free oscillations (Sect. 5), which must use time windows of several weeks to obtain a proper sampling of their spectra (DAHLEN, 1982).

2. Mantle Magnitude M_m from Ultra-Long Period Rayleigh Waves

In this section, we extend to ultra-long periods (reaching 550 s) the concept of the mantle magnitude M_m developed by OKAL and TALANDIER (1989). We recall that it consists of interpreting the spectral amplitudes $X(\omega)$ of mantle Rayleigh waves, to infer a seismic moment M_0 using the philosophy of a *magnitude* scale, i.e., neglecting the influence of focal mechanism and depth. M_m , defined as

$$M_m = \log_{10} M_0 - 20 = \log_{10} X(\omega) + C_S + C_D + C_0, \quad (1)$$

uses an exact distance correction C_D and scaling constant C_0 , but an average source correction, C_S , derived theoretically in the framework of normal mode theory. This concept has been at the root of the TREMORS detection and quantification algorithm used at the Papeete Warning Center (REYMOND *et al.*, 1993). In practice, the M_m algorithm has been run on periods not exceeding 300 s.

With the generalization of very-broadband instrumentation, it becomes feasible to extend M_m to ultra-long periods, in practice reaching 550 s. At the very long periods involved ($300 \text{ s} \leq T \leq 550 \text{ s}$), the regionalization of the Earth used in the computation of C_D (OKAL and TALANDIER, 1989) becomes largely

irrelevant, and a single Earth model can be used. Further, we have verified that the spline used to derive C_S as an average value of the true excitation of the Rayleigh waves, remains valid within 0.15 logarithmic units. It then becomes straightforward to extend OKAL and TALANDIER'S (1989) algorithm to periods as long as 550 s.

In the hours following the 2011 Tohoku earthquake, records were processed from first passages R_1 at 63 stations of the Incorporated Research Institutions for Seismology (IRIS) global network, and spectral amplitudes converted into M_m values. Results are plotted as the individual solid dots on Fig. 1. At each of the 30 frequencies used, we then averaged the values of M_m over all 63 stations, with the results shown as the open and colored circles on Fig. 1. In principle, the values of M_m should be independent of period if the source was a perfect δ -function in time and space. However, and as expected, the station-averaged values show a tendency to grow with period, reflecting the destructive interference provoked in the high-frequency spectrum by source finiteness, a classical effect first described by BEN-MENACHEM (1961), and which incidentally is the cause of the saturation of all classical magnitudes (GELLER, 1976). Any source slowness in the low-frequency part of the spectrum, over and beyond what would be expected from scaling laws, will increase this effect at the lowest frequencies. We explore any such possible trend by regressing the station-averaged values against frequency as

$$M_m = a - bf \quad (2)$$

in two frequency bands: $f = 0$ (in practice 1.8) to 5 mHz (red points on Fig. 1) and $f = 5$ to 10 mHz (green points in Fig. 1), and we compare the slopes of the regressions by forming their ratio $R = b_{0-5}/b_{5-10}$. These results are listed in Table 1, and compared to their counterparts for large recent events, and smaller "tsunami earthquakes" featuring source slowness. All events used in Table 1 generated destructive tsunamis, in the near or far field. The population of ratios R shows an essentially bimodal distribution: a first group of events, including the large 2010 Maule, Chile earthquake, feature a ratio of ~ 1 , meaning that there is essentially no difference in the evolution of their spectra in the two frequency bands. A second

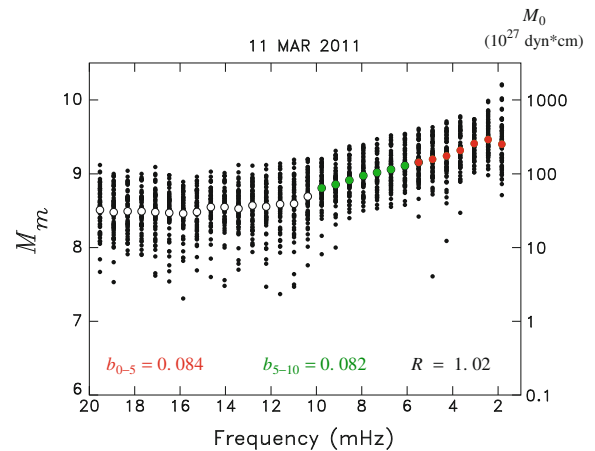


Figure 1
Individual measurements of M_m taken in real time in the aftermath of the 2011 Tohoku earthquake. At each frequency, the larger symbols are values averaged over all stations. The slopes of regressions taken below 5 mHz (red) and between 5 and 10 mHz (green) are given at the bottom of the figure, as well as the ratio of the two numbers

group features ratios R on the order of 2 or more, meaning that the growth of moment with period accelerates above 200 s of period (Fig. 2). The four classical "tsunami earthquakes" of the past 20 years belong to this group, as does the 2004 Sumatra event. All these earthquakes have been shown to feature source slowness, expressed, for example, by deficient energy-to-moment ratios (see Sect. 3).

The 2011 Tohoku earthquake clearly belongs to the first group, and thus features no intrinsic source slowness. The nearly identical parameters $a_{5-10} = 9.61$ and $a_{0-5} = 9.62$ in (2) provide estimates of the static moment of the event (4.11 and 4.15×10^{29} dyn cm, respectively), which agree remarkably well with the real-time solution (4×10^{29} dyn cm) provided around 06:30 UTC by the NEIC using the W -phase inversion algorithm (DUPUTEL *et al.*, 2011).

3. Energy-to-Moment Ratio and Slowness Parameter Θ

In this section, we apply NEWMAN and OKAL'S (1998) algorithm to compute the slowness parameter

Table 1
Regression parameters of M_m versus frequency

Date	Region	Moment (10^{27} dyn cm)	Slope b_{5-10}	Slope b_{0-5}	Ratio R
<i>Regular sources</i>					
15 NOV (319) 2006	Kuril	34.0	0.074	0.069	0.93
12 SEP (255) 2007	Bengkulu	51.0	0.079	0.089	1.13
29 SEP (272) 2009	Samoa	12.0	0.062	0.046	0.75
27 FEB (058) 2010	Maule	185.0	0.103	0.097	0.94
11 MAR (070) 2011	Tohoku	400.0	0.083	0.085	1.02
<i>Slow sources</i>					
02 SEP (246) 1992	Nicaragua	3.4	0.058	0.105	1.81
02 JUN (153) 1994	Java	5.3	0.026	0.074	2.84
21 FEB (052) 1996	Chimbote, Peru	2.2	0.031	0.081	2.61
26 DEC (361) 2004	Sumatra	1150.0	0.068	0.243	3.60
17 JUL (198) 2006	Java	4.0	0.007	0.074	10.15

The units of the slopes b are logarithmic units of magnitude M_m per mHz

$$\Theta = -\log_{10} \frac{E^E}{M_0} \quad (3)$$

characterizing the ratio of the estimated energy of the source, E^E , to the seismic moment M_0 . We recall that this approach is inspired by BOATWRIGHT and CHOY'S (1986) computation of the seismic energy radiated by the body waves, but E^E in (3) keeps the philosophy of a *magnitude* measurement, ignoring the specific details of focal mechanism and source depth, often unavailable or poorly constrained in real time. Θ expresses a ratio between a high-frequency property of the source (E^E) and a low-frequency one (M_0), which, under scaling laws, should be an invariant (theoretically predicted to take the value -4.90). In general, large megathrust earthquakes exhibit a trend towards slowness ($-5.5 \leq \Theta \leq -5.0$), including the 2010 Maule earthquake ($\Theta = -5.35$). By contrast, any deviation from such values is a proxy for an anomalous source spectrum, and thus a violation of scaling laws. In particular, all "tsunami earthquakes" have been found to feature Θ deficient by at least one logarithmic unit ($\Theta \leq -5.9$), as did the 2004 Sumatra earthquake ($\Theta = -6.40$). On the other hand, values of Θ significantly greater than predicted are the trademark of "snappy" events featuring high stress drops, such as the 2011 Christchurch earthquake ($\Theta = -4.19$), or other intraplate events (triangles on Fig. 3).

Figure 3 presents the results of our real-time analysis of generalized P wavetrains at 32 stations, yielding $\Theta = -5.65$. We note that this value features a trend towards slowness which is stronger than typical of interplate thrust earthquakes, but it fails to qualify the event as truly slow. In this respect, and as documented on Fig. 3, the 2011 Tohoku event remains comparable to such events as 2010 Maule ($\Theta = -5.35$), Nias 2005 ($\Theta = -5.54$), Bengkulu 2007 ($\Theta = -5.78$) or 2001 Peru ($\Theta = -5.65$), none of which featured source slowness (as discussed by WEINSTEIN and OKAL (2005), the latter had a delayed, rather than slow, source), nor anomalous tsunamis.

4. Duration of High-Frequency P Waves

This section uses high-frequency P waves to recover an estimate of the duration of faulting at the source. In the aftermath of the 2004 Sumatra event, NI *et al.* (2005) remarked that, due to the attenuation properties of the mantle, direct P waves were, in general, the only phase capable of transmitting very high frequency energy to distant stations. Thus, upon drastic filtering (e.g., in the range $2 \leq f \leq 4$ Hz), the only phase remaining in a teleseismic signal will be the P wave, and an analysis of its duration can be carried out without contamination by other phases such as PP or S , which could interfere with P in the

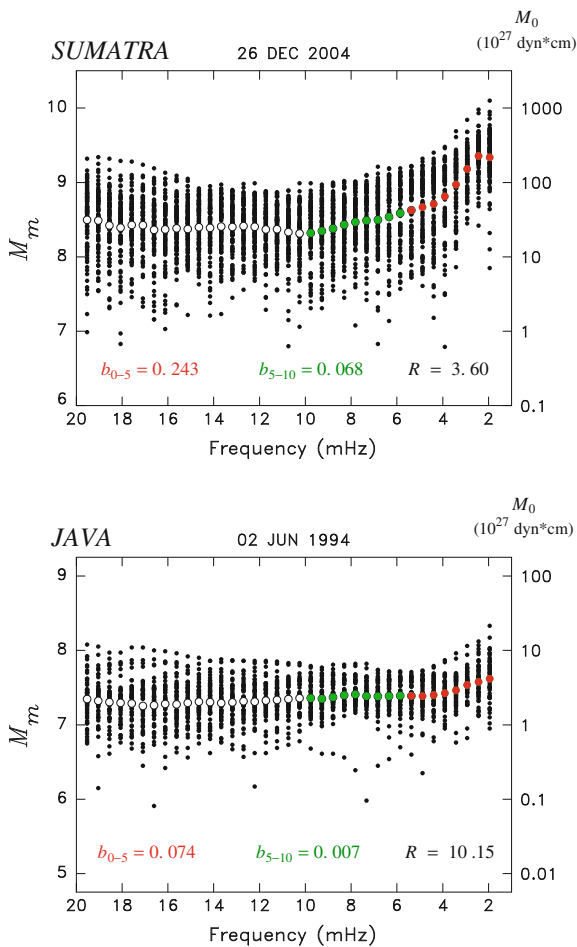


Figure 2

Same as Fig. 1 for the 2004 Sumatra (Top) and 1994 Java (Bottom) events. Contrary to the case of the Tohoku earthquake, these slow events feature a spectrum growing fast below 5 mHz, leading to ratios R much in excess of 1

case of extremely long sources, such as the 2004 Sumatra earthquake.

Under scaling laws, the duration of rupture τ , controlled by fault length L and rupture velocity v_R , is expected to grow like $M_0^{1/3}$, and the ratio of those two quantities should be an invariant of the source, controlled by the medium rigidity μ , the strain release ε , and v_R , all of which should be size-independent properties.

We obtain an estimate of τ by constructing an envelope of the filtered ground-velocity times series, and measuring the time $\tau_{1/3}$ during which the amplitude of the envelope remains above 1/3 of its maximum value. This methodology is inspired (with

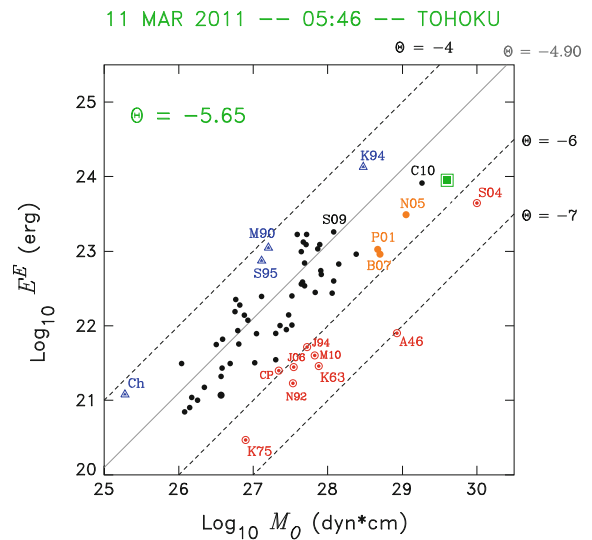


Figure 3

Estimated Energy E^E versus moment M_0 for a background of ~ 90 large earthquakes of past 35 years. Lines of constant Θ are shown as dashed lines, with the solid grey line representing the theoretical value (-4.90) expected from scaling laws. The 2011 Tohoku event is shown as the large square symbol. The circular bull's eyes identify the "tsunami earthquakes" with $\Theta < -5.80$. By contrast, the triangles identify "snappy" earthquakes with $\Theta > -4.3$. Relevant earthquakes are identified as: A46, Unimak 1946; B07, Bengkulu 2007; C10, Chile 2010; Ch, Christchurch 2011; CP, Chimbote, Peru 1996; J94, Java 1994; J06, Java 2006; K63, Kuril 1963 (20 Oct.); K75, Kuril 1975; K94, Kuril 1994; M90, Marianas 1990; M10, Mentawai 2010; N05, Nias 2005; N92, Nicaragua 1992; P01, Peru 2001; S95, Samoa 1995; S04, Sumatra 2004; and S09, Samoa, 2009

only slightly different parameterization) by TALANDIER and OKAL'S (2001) discriminant D for explosive sources of hydroacoustic energy recorded at T -phase stations, and the reader is referred to this work for details of the procedure. An example of measurement is given in Fig. 4.

When averaged over a dataset of 40 stations, the mean $\overline{\tau_{1/3}} = 65$ s is found to be substantially smaller than the true duration of rupture, as resolved, for example, by source tomography studies. This reflects in particular the strong directivity effects resulting from the spatial distribution of the departing rays (GELLER, 1976). In this respect, $\tau_{1/3}$ cannot be directly interpretable as the rupture time L / v_R of the source, but its measure provides a robust way to compare the relative time intervals over which a variety of events have generated high-frequency waves into the Earth. Figure 5 shows that the 2011 Tohoku earthquake

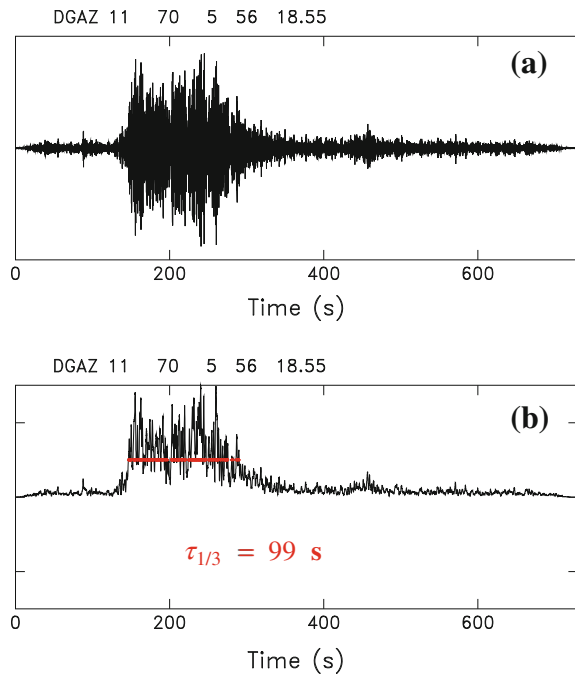


Figure 4

Principle of the measure of $\tau_{1/3}$. **a** Broad-band seismogram of the 2011 Tohoku earthquake at Diego Garcia (DGAR), band-pass filtered between 2 and 4 Hz. Note that this procedure eliminates all phases other than P . **b** Envelope of **(a)**, using the procedure of TALANDIER and OKAL (2001). The *thick line* represents the fraction of the record for which the envelope remains above 1/3 of its maximum value. Its length defines $\tau_{1/3}$

appears, if anything, shorter in duration than average, and certainly does not share the excessive $\tau_{1/3}/M_0$ ratio systematically featured by tsunami earthquakes and other slow sources.

An alternate way of interpreting the previous results is to combine the measurement of $\tau_{1/3}$ and E^E , through the quantity

$$\Phi = \log_{10} \tau_{1/3} - \frac{1}{3} \log_{10} E^E + 5.86, \quad (4)$$

where the last constant has been adjusted to give Φ a zero mean over a large background dataset of about 60 earthquakes. This procedure eliminates the long-period moment M_0 . A slow source will have both a deficient E^E and a prolonged $\tau_{1/3}$, hence a large positive Φ , typically greater than 0.35. This is the case of all “tsunami earthquakes” ($0.46 \leq \Phi \leq 1.08$; Fig. 6), but not of the 2004 Sumatra earthquake, which has only $\Phi = 0.22$, probably reflecting an only moderately slow rupture velocity of 2.5 km/s (e.g.,

GUILBERT *et al.*, 2005; ISHII *et al.*, 2005), as opposed to as low as 0.9 km/s for the typical “tsunami earthquakes” (POLET and KANAMORI, 2000). (In addition, the $\tau_{1/3}$ algorithm cannot catch a very long source whose last portions may have a diminished amplitude, falling below the 1/3 threshold, which contributes to a limitation on the parameter Φ for this exceptional event.)

For the 2011 Tohoku event, we obtain $\Phi = -0.31$, confirming the relatively fast character of its source (Fig. 6).

Note that the computation of Φ is conceptually related to the inverse of the discriminant E/T_R^3 recently introduced by NEWMAN *et al.* (2011) and implemented as part of their automated evaluator of source slowness, although the parameters computed, E^E versus E and $\tau_{1/3}$ versus T_R , are not exactly identical. Nevertheless, it is interesting to note that we find a difference of 0.70 units in Φ between the slow 2010 Mentawai “tsunami earthquake” ($\Phi = 0.39$), and the 2011 Tohoku event, whereas NEWMAN *et al.*’s dataset would suggest a very similar difference of 0.64 units.

5. Quantification of Normal Modes Excited by the 2011 Tohoku Earthquake

In this section, we explore in a definitive fashion the low-frequency end of the source spectrum of the 2011 Tohoku earthquake by quantifying the amplitude of the Earth’s spheroidal free oscillations that it excited. Whereas all previous measurements (Sects. 2–4) could be made in real-time operational mode and contributed to the tsunami alert during the night of 10–11 March (local time) at the Laboratoire de Géophysique in Tahiti, the investigation of the modes had to be deferred until sufficiently long time series became available (DAHLEN, 1982).

Our study matches the amplitude of observed spectral lines of the various modes to theoretical spectra computed in the formalism of STEIN and GELLER (1977), which allows the precise modeling of the excitation, by a source of any geometry, of each of the $(2l + 1)$ singlets ${}_nS_l^m$, where the individual mode ${}_nS_l$ has been split by the Earth’s rotation and ellipticity. It follows in the footsteps of our previous work on the normal modes of the 2004 Sumatra, 2005

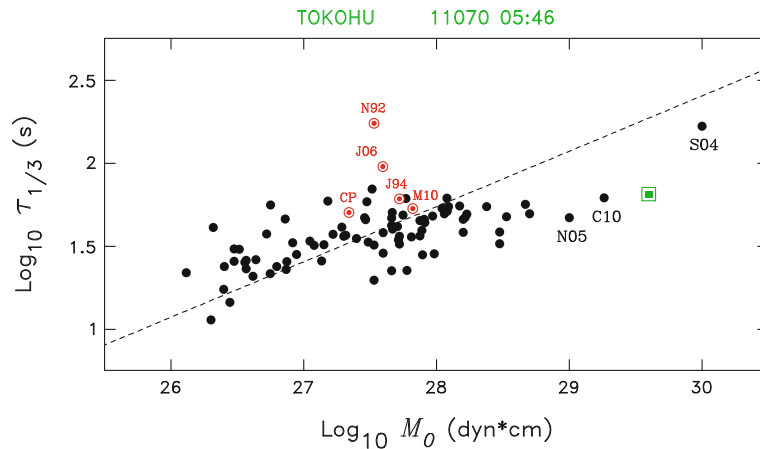


Figure 5

Results of the measurement of $\tau_{1/3}$ compared to a background of values for other events. The *dashed line* best fits that dataset under the assumption of a constant ratio between $\tau_{1/3}$ and $M_0^{1/3}$, as predicted by scaling laws. Note that the “tsunami earthquakes”, identified by *bull’s eye symbols*, all plot above the *line*. The 2011 Tohoku event is shown as the *large square*. Event codes as in Fig. 3

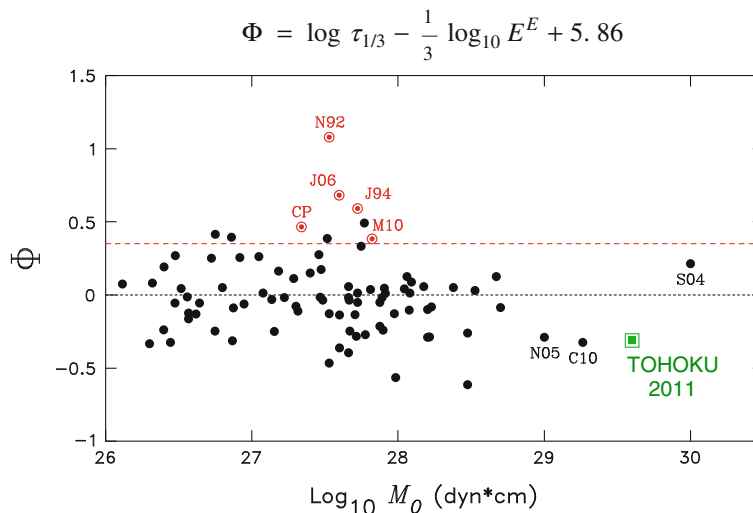


Figure 6

Parameter Φ plotted versus moment, for a dataset of ~ 60 background earthquakes. This parameter is designed to emphasize source slowness, and is computed exclusively from P waves. The long-dashed line is the threshold (0.35) above which events feature excessive slowness, including all “tsunami earthquakes”. By contrast, the 2011 Tohoku earthquake shows a negative Φ . Earthquake codes as in Fig. 3

Nias, and 2010 Maule earthquakes, as described in STEIN and OKAL (2005, 2007) and OKAL *et al.* (2012), to which the reader is referred for all details of the computational procedures.

In practice, we were able to model the fundamental spheroidal modes ${}_0S_2$ to ${}_0S_5$, the overtones ${}_1S_3$ and ${}_1S_4$, and the radial modes ${}_0S_0$ and ${}_1S_0$. In the case of ${}_1S_3$, we included the contribution of ${}_3S_1$, which has a similar eigenfrequency, to the extent that the two

groups of singlets cannot be separated. We found the spectra of the torsional modes too noisy to be processed. We used exclusively continuous time windows, lasting an average of 20 days, except for ${}_0S_0$ for which we used 75-day-long windows, on account of the exceptionally high Q of the mode. As a whole, we obtained 117 fits for eight multiplets. Figures 7 and 8 give representative examples of the spectral lines and their theoretical fits.

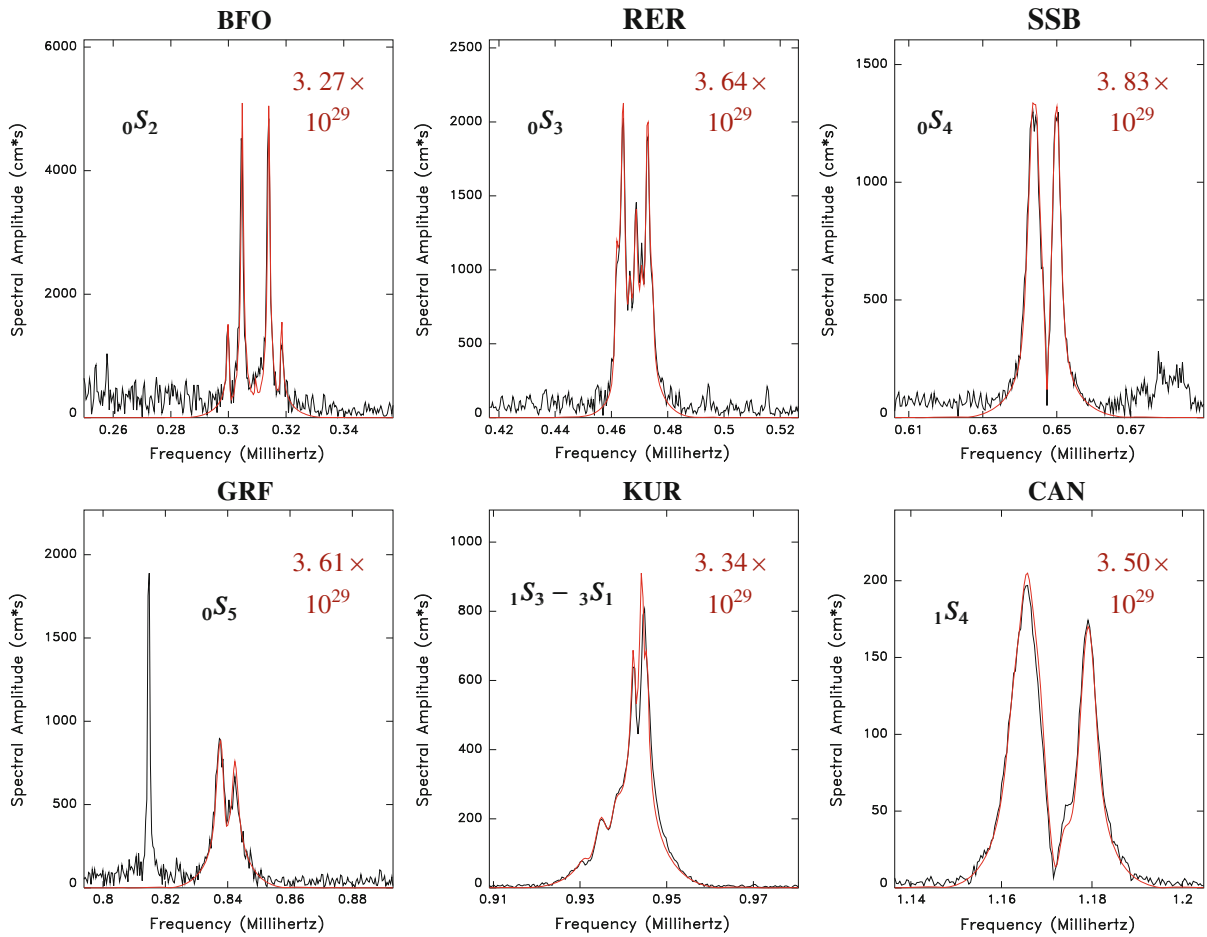


Figure 7

Examples of spheroidal mode fits. For each mode, a representative station (with *three letter code*) is used. The *black trace* is the spectral amplitude of vertical ground motion in a narrow window centered on the mode. The *red trace* is the theoretical spectrum, computed using STEIN and GELLER'S (1977) algorithm. The moment value, printed at *upper right* in each frame, is obtained by best-fitting the two curves. In the case of ${}_0S_5$, the *narrow spectral line at left* is the radial mode ${}_0S_0$ (see Fig. 8), located outside the best-fitting window

The normal mode results are summarized in Table 2, and plotted on Fig. 9. Over the range of periods studied, we find an essentially flat spectrum. With the exception of the duo ${}_1S_3 - {}_3S_1$, which only grazes it, all error bars of the individual modes fit the $1-\sigma$ band about the geometrically averaged moment of 3.54×10^{29} dyn cm. Most importantly, we fail to identify any trend of an increase of moment with periods; if anything, the moments computed decrease slightly with increasing period, the best-fitting logarithmic slope being -0.004 , an insignificant number as compared with the positive value of $+0.39$ found for the 2004 Sumatra earthquake (STEIN and OKAL, 2007).

6. Discussion and Conclusion

We have presented a total of five methodologies, using the whole spectrum of teleseismic waves over a range of frequencies covering four order of magnitudes, from the 3-Hz *P* waves used to compute $\tau_{1/3}$ to 0.3 mHz for ${}_0S_2$. All attempts fail to document any slowness in the source of the 2011 Tohoku event, in the sense of a growth of its source spectrum with increasing period.

Beyond the gravest Earth mode, seismological methods are powerless to resolve the source spectrum, but we note the work of HAN *et al.* (2011), who

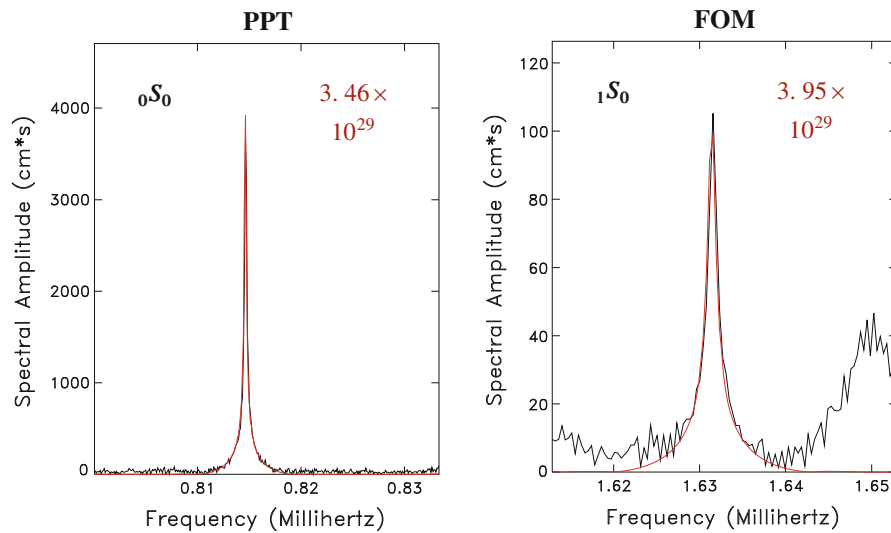


Figure 8
Same as Fig. 7 for the radial modes ${}_0S_0$ and ${}_1S_0$

Table 2
Results of the normal mode analysis

Mode	Period (s)	Best-fitting moment		
		M_0 (10^{29} dyn cm)	Standard deviation (%)	Number of stations
${}_0S_2$	3,232	3.39	1.03	8
${}_0S_3$	2,134	3.55	1.07	19
${}_0S_4$	1,545	3.72	1.06	16
${}_0S_5$	1,190	3.47	1.07	15
${}_1S_3 - {}_3S_1$	1,062	3.02	1.07	15
${}_1S_4$	852	3.63	1.11	15
${}_0S_0$	1,227	3.39	1.06	11
${}_1S_0$	613	3.89	1.07	18
Average		3.54	1.07	117

The standard deviation is given as a multiplicative or divisive factor (%)

mapped deformations of the GRACE satellite orbits into a dataset of spherical harmonics expansions of the perturbations of the gravity potential of the Earth due to the earthquake. These can be described as “static” although more precisely, they correspond to a period of ~ 3 weeks, representing the time over which the orbits were studied. In turn, HAN *et al.* (2011) were able to invert this dataset into a moment tensor. While their scalar moment trades off with other parameters such as depth and fault dip, the values of M_0 fall between 4 and 5×10^{29} dyn cm,

comparable to the range of seismic solutions published in the aftermath of the event, e.g., the W -phase estimate of 4×10^{29} or the final Global CMT solution of 5.3×10^{29} dyn cm.

This is not to say that the 2011 Tohoku earthquake had a “textbook” source. Most source tomographic studies have proposed a patch of extreme slip reaching locally anywhere from 40 to 70 m (e.g., LAY *et al.*, 2011), over a reduced area not exceeding 200 by 100 km, which implies strains of 5×10^{-4} , in excess of commonly accepted values for what should be an invariant of the source. This in itself constitutes a violation of scaling laws.

However, our results indicate that, at the ultra-low frequency end of the seismic spectrum, the 2011 Tohoku earthquake had no hidden low-frequency component escaping detection under traditional seismological techniques. In this respect, the 2011 event is most reminiscent of the 2010 Maule and 2005 Nias earthquakes, and differs significantly from the 2004 Sumatra earthquake, whose gravest normal modes were excited by a moment ~ 3 times larger than its CMT solution.

Among historical earthquakes, and as mentioned earlier, the 1960 Chile earthquake and the smaller 1946 Unimak event (LÓPEZ and OKAL, 2006) had strong low-frequency components, a behavior shared (on a somewhat smaller scale) by the 1964 Alaska earthquake (NETTLES *et al.*, 2005). Preliminary evidence of deficient high-frequency body-wave energy

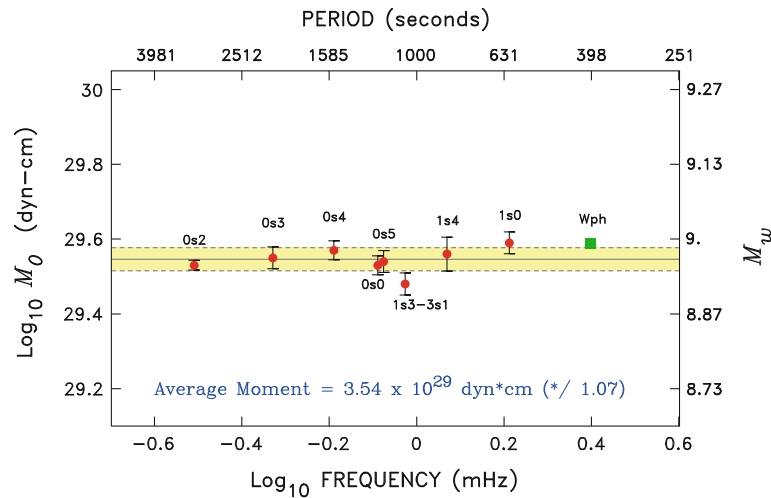


Figure 9

Results from the quantification of six spheroidal and two radial modes. For each mode, the best-fitting moment has been geometrically averaged over all contributing stations, and is shown as a *solid dot*, with its standard deviation *bar*. The *gray line* is the final averaged moment from the mode study, and the shaded band its one- σ confidence interval. The solid square is the moment obtained in real time by inversion of *W* phases (DUPUTEL *et al.*, 2011)

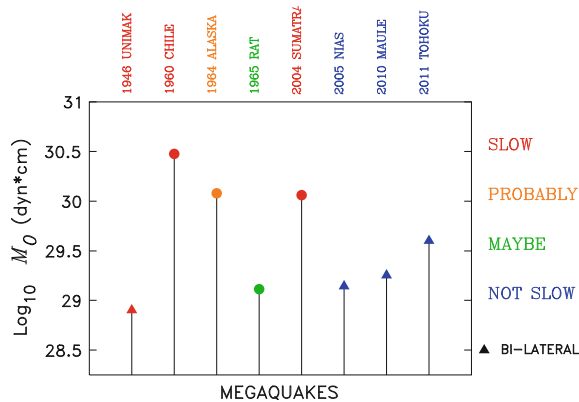


Figure 10

Sketch of the moments of seven mega earthquakes (plus the 1946 Unimak event) of the past 66 years. The *vertical bars* are scaled (logarithmically) to moment, and the events *color-coded* according to the presence or absence of slowness in their source. Events featuring bi-lateral rupture are shown as *triangles*

indicates that the 1965 Rat Island earthquake may also feature slowness in its source.

These results are sketched on Fig. 10, which would suggest that the three “super-mega” earthquakes ($M_0 \geq 10^{30}$ dyn cm) are all slow, while the next tier (Tohoku, Maule, Nias) are regular. We also note that these latter three events all had significantly bilateral ruptures. But such apparent trends are violated by the very slow, bilateral Unimak source, and

if its slowness could be confirmed, by the Rat Island earthquake, which belongs to the second tier in terms of moment. Given the scarcity of the dataset of mega earthquakes, it is clear that detailed investigation of historical events for which modern low-frequency solutions are not available (e.g., 1950 Assam, 1952 Kamchatka, 1957 Aleutian) would be highly desirable. Only then (and if more mega events occur in the not too distant future), will we be able to unravel the mystery of slow components of mega earthquakes.

Acknowledgments

I thank Dominique Reymond and Olivier Hyvernaud, with whom I shared the intense night of 10 March 2011 at the Laboratoire de Géophysique in Papeete. The mode-splitting codes were originally written 35 years ago by Seth Stein.

REFERENCES

- AKI, K. (1967), *Scaling law of seismic spectrum*, J. Geophys. Res., 72, 1217–1231.
- BEN-MENACHEM, A. (1961), *Radiation of seismic surface-waves from finite moving sources*, Bull. Seismol. Soc. Amer., 51, 401–435.
- BOATWRIGHT, J., and G.L. CHOY (1986), *Teleseismic estimates of the energy radiated by shallow earthquakes*, J. Geophys. Res., 91, 2095–2112.

- CHOY, G.L., and J. BOATWRIGHT (2007), *The energy radiated by the 26 December 2004 Sumatra-Andaman earthquake estimated from 10-minute P -wave windows*, Bull. Seismol. Soc. Amer., 97, S18–S24.
- CIFUENTES, I.L., and P.G. SILVER (1989), *Low-frequency source characteristics of the great 1960 Chilean earthquake*, J. Geophys. Res., 94, 643–663.
- DAHLEN, F.A. (1982), *The effect of data windows on the estimation of free oscillation parameters*, Geophys. J. Roy. astr. Soc., 69, 537–549.
- DUPUTEL, Z., L. RIVERA, H. KANAMORI, G. HAYES, B. HIRSHORN, and S. WEINSTEIN (2011), *Real-time W -phase inversion during the 2011 Tohoku earthquake*, Earth, Planets, Space, 63, 535–539.
- FUKAO, Y. (1979), *Tsunami earthquakes and subduction processes near deep-sea trenches*, J. Geophys. Res., 84, 2303–2314.
- GELLER, R.J. (1976), *Scaling relations for earthquake source parameters and magnitudes*, Bull. Seismol. Soc. Amer., 66, 1501–1523.
- GUILBERT, J., J. VERGOZ, E. SCHISSELÉ, A. ROUEFF, and Y. CANSI (2005), *Use of hydroacoustic and seismic arrays to observe rupture propagation and source extent of the $M_w = 9.0$ Sumatra earthquake*, Geophys. Res. Letts., 32, (15), L15310.
- GUTENBERG, B., and C.F. RICHTER, *Seismicity of the Earth and associated phenomena* (Princeton University Press, 310 pp., 1954).
- HAN, S.-C., J. SAUBER, and R.E.M. RIVA (2011), *Contribution of satellite gravimetry to understanding seismic source processes of the 2011 Tohoku-Oki earthquake, and focal mechanism*, Geophys. Res. Letts., 38, (24), L24312.
- IDE, S., and G.C. BEROZA (2001), *Does apparent stress vary with earthquake size?* Geophys., Res. Letts., 28, 3349–3352.
- ISHII, M., P.M. SHEARER, H. HOUSTON, and J.E. VIDALE (2005), *Extent, duration and speed of the 2004 Sumatra-Andaman earthquake, imaged by the Hi-Net array*, Nature, 435, 933–936.
- KANAMORI, H. (1972), *Mechanism of tsunami earthquakes*, Phys. Earth Planet. Inter., 6, 346–359.
- KANAMORI, H., and D.L. ANDERSON (1975), *Amplitude of the Earth's free oscillations and long-period characteristics of the earthquake source*, J. Geophys. Res., 80, 1075–1078.
- KANAMORI, H., and J.J. CIPAR (1974), *Focal process of the great Chilean earthquake, May 22, 1960*, Phys. Earth Planet. Inter., 9, 128–136.
- LAY, T., and S.L. BILEK, *Anomalous earthquake ruptures at shallow depths on subduction zone megathrusts*, in: *The seismogenic zone of subduction thrust faults* (Eds. T. DIXON and C. MOORE, Columbia Univ. Press, New York, 2007) pp. 476–511.
- LAY, T., C.J. AMMON, H. KANAMORI, L. XUE, and M.J. KIM (2011), *Possible large near-trench slip during the 2011 $M_w = 9.0$ Tohoku earthquake*, Earth Planets Space, 63, 687–692.
- LINDE, A.T., and P.G. SILVER (1989), *Elevation changes and the great 1960 Chilean earthquake: Support for aseismic slip*, Geophys. Res. Letts., 16, 1305–1308.
- LÓPEZ, A.M., and E.A. OKAL (2006), *A seismological reassessment of the source of the 1946 Aleutian "tsunami" earthquake*, Geophys. J. Intl., 165, 835–849.
- NETTLES, M., G. EKSTRÖM, A.M. DZIEWOŃSKI, and N. MATERNOVSKAYA (2005), *Source characteristics of the great Sumatra earthquake and its aftershocks*, Eos, Trans. Amer. Geophys. Un., 86, (18), U43A-01 [abstract].
- NEWMAN, A.V., and E.A. OKAL (1998), *Teleseismic estimates of radiated seismic energy: The E/M_0 discriminant for tsunami earthquakes*, J. Geophys. Res., 103, 26885–26898.
- NEWMAN, A.V., G. HAYES, Y. WEI, and J.A. CONVERS (2011), *The 25 October 2010 Mentawai tsunami earthquake, from real-time discriminants, finite-fault rupture, and tsunami excitation*, Geophys. Res. Letts., 38, (5), L05302.
- Ni, S., H. KANAMORI, and D.V. HELMBERGER (2005), *Energy radiation from the Sumatra earthquake*, Nature, 434, 582.
- OKAL, E.A. (2011), *Lessons from Sendai: A perspective from Polynesia and the world*, Geophys. Res. Abstracts, 13, EGU2011-14228.
- OKAL, E.A., and J. TALANDIER (1989), *M_m : A variable period mantle magnitude*, J. Geophys. Res., 94, 4169–4193.
- OKAL, E.A., S. HONGRESAWAT, and S. STEIN (2012), *Split mode evidence for no ultra-slow component to the source of the 2010 Maule, Chile earthquake*, Bull. Seismol. Soc. Amer., 102, 391–397.
- POLET, J., and H. KANAMORI (2000), *Shallow subduction zone earthquakes and their tsunamigenic potential*, Geophys. J. Intl., 142, 684–702.
- REYMOND, D., O. HYVERNAUD, and J. TALANDIER, *An integrated system for real-time estimation of seismic source parameters, and its application to tsunami warning*, In: *Tsunamis in the World* (ed. S. Tinti, Kluwer, Dordrecht, 1993) pp. 177–196.
- REYMOND, D., O. HYVERNAUD, and E.A. OKAL (2012), *The 2010 and 2011 tsunamis in French Polynesia: Operational aspects and field surveys*, Pure Appl. Geophys., doi:10.1007/s00024-012-0485-5.
- RUNDLE, J.B. (1989), *Derivation of the complete Gutenberg–Richter magnitude–frequency relation using the principle of scale invariance*, J. Geophys. Res., 94, 12337–12342.
- STEIN, S., and R.J. GELLER (1977), *Amplitudes of the Earth's split normal modes*, J. Phys. Earth, 25, 117–142.
- STEIN, S., and E.A. OKAL (2005), *Size and speed of the Sumatra earthquake*, Nature, 434, 581–582.
- STEIN, S., and E.A. OKAL (2007), *Ultra-long period seismic study of the December 2004 Indian Ocean earthquake and implications for regional tectonics and the subduction process*, Bull. Seismol. Soc. Amer., 97, S279–S295.
- TALANDIER, J., and E.A. OKAL (2001), *Identification criteria for sources of T waves recorded in French Polynesia*, Pure Appl. Geophys., 158, 567–603.
- TANIOKA, Y., L.J. RUFF, and K. SATAKE (1997), *What controls the lateral variation of large earthquake occurrence along the Japan trench?*, Island Arc, 6, 261–266.
- TSAI, V.C., M. NETTLES, G. EKSTRÖM, and A.M. DZIEWOŃSKI (2005), *Multiple CMT source analysis of the 2004 Sumatra earthquake*, Geophys. Res. Letts., 32, (17), L17304.
- WEINSTEIN, S.A., and E.A. OKAL (2005), *The mantle wave magnitude M_m and the slowness parameter Θ : Five years of real-time use in the context of tsunami warning*, Bull. Seismol. Soc. Amer., 95, 779–799.